JOURNAL OF VIROLOGY, Mar. 1996, p. 1714–1722 Vol. 70, No. 3
0022-538X/96/$04.00+0


# Disruption of Prion Rods Generates 10-nm Spherical Particles Having High α-Helical Content and Lacking Scrapie Infectivity

DETLEV RIESNER,[1]* KLAUS KELLINGS,[1] KARIN POST,[1] HOLGER WILLE,[2] HANA SERBAN,[2] DARLENE GROTH,[2] MICHAEL A. BALDWIN,[2] AND STANLEY B. PRUSINER[2,3]

*Institut für Physikalische Biologie und Biologisch-Medizinisches Forschungszentrum, Heinrich-Heine-Universität Düsseldorf, 40225 Düsseldorf, Germany,[1] and Departments of Neurology[2] and Biochemistry and Biophysics,[3] University of California, San Francisco, California 94143-0518*

Received 26 July 1995/Accepted 30 November 1995

**An abnormal isoform of the prion protein (PrP) designated $PrP^{Sc}$ is the major, or possibly the only, component of infectious prions. Structural studies of $PrP^{Sc}$ have been impeded by its lack of solubility under conditions in which infectivity is retained. Among the many detergents examined, only treatment with the ionic detergent sodium dodecyl sulfate (SDS) or Sarkosyl followed by sonication dispersed prion rods which are composed of PrP 27-30, an N-terminally truncated form of $PrP^{Sc}$. After ultracentrifugation at 100,000 × *g* for 1 h, ~30% of the PrP 27-30 and scrapie infectivity were found in the supernatant, which was fractionated by sedimentation through 5 to 20% sucrose gradients. Near the top of the gradient, spherical particles with an observed sedimentation coefficient of ~6S, ~10 nm in diameter and composed of four to six PrP 27-30 molecules, were found. The spheres could be digested with proteinase K and exhibited little, if any, scrapie infectivity. When the prion rods were disrupted in SDS and the entire sample was fractionated by sucrose gradient centrifugation, a lipid-rich fraction at the meniscus composed of fragments of rods and heterogeneous particles containing high levels of prion infectivity was found. Fractions adjacent to the meniscus also contained spherical particles. Circular dichroism of the spheres revealed 60% α-helical content; addition of 25% acetonitrile induced aggregates high in β sheet but remaining devoid of infectivity. Although the highly purified spherical oligomers of PrP 27-30 lack infectivity, they may provide an excellent substrate for determining conditions of renaturation under which prion particles regain infectivity.**

The prion diseases include Creutzfeldt-Jakob disease of humans as well as scrapie of sheep and bovine spongiform encephalopathy (8, 30, 31, 51). The human prion diseases are manifest as familial, sporadic, and infectious illnesses; the inherited disorders are caused by mutations of the prion protein (PrP) gene on chromosome 20 which result in nonconservative amino acid substitutions (for a review, see reference 33). Prions are proteinaceous, infectious particles that are composed largely, if not entirely, of an abnormal PrP isoform designated $PrP^{Sc}$. Both $PrP^{Sc}$ and the cellular isoform $PrP^{C}$ are encoded by the PrP gene; $PrP^{Sc}$ is derived from $PrP^{C}$ by a posttranslational process (for a review, see reference 32). Limited proteolysis of $PrP^{Sc}$ produces an N-terminally truncated protein designated PrP 27-30 under conditions in which prion infectivity is retained. PrP 27-30 forms rod-shaped polymers with the tinctorial properties of amyloid that are referred to as prion rods (38).

The transformation of $PrP^{C}$ into $PrP^{Sc}$ involves a profound conformational change. $PrP^{C}$ is predominantly an α-helical protein, whereas $PrP^{Sc}$ exhibits substantial β sheet and reduced amounts of α helix (29, 42). Treatment of $PrP^{Sc}$ with solvents such as hexafluoroisopropanol (HFIP) increased the α-helix content of $PrP^{Sc}$ and resulted in a substantial reduction in scrapie infectivity (9, 43). Attempts to identify a chemical modification or auxiliary molecule that induces this conformational change have been unrewarding. Analysis of peptides generated from denatured $PrP^{Sc}$ by limited proteolysis failed to identify any candidate covalent modification that might be responsible for such a shift in tertiary structure (46). Despite an intensive search for a second component such as a scrapie-specific nucleic acid, none has been found; quantitative analyses of residual nucleic acids have eliminated oligonucleotides greater than ~80 nucleotides in length (15, 40).

Conformational studies of the PrP isoforms are complicated by the differences in solubility of these proteins. For example, $PrP^{C}$ is soluble in nondenaturing detergents whereas $PrP^{Sc}$ is not (21). To obtain high-resolution structural data, conditions for solubilization of $PrP^{Sc}$ under which scrapie prion infectivity is retained need to be identified. Early attempts to solubilize scrapie infectivity (23) were unsuccessful, and the insolubility of the infectious particles retarded development of effective purification protocols (37, 44). Once the insolubility of scrapie infectivity was appreciated, it was used to enrich fractions for infectivity, which led to the discovery of PrP 27-30 (34). Some investigators were misled by the assumption that scrapie is caused by a virus and that the smallest infectious scrapie particles were likely to be quite large (16), despite ionizing radiation data to the contrary (1).

Solubilization of $PrP^{Sc}$ and PrP 27-30 was effected when they were mixed with phospholipids to form liposomes or detergent-lipid-protein complexes (7). The use of phospholipids to solubilize scrapie prions has not been helpful in structural studies of the prion proteins because such high concentrations of lipid are required. In some investigations, scrapie infectivity was reported to have observed sedimentation values as low as 2 to 3S (19). Recent claims that prion infectivity can be recovered from sodium dodecyl sulfate (SDS)-polyacrylamide gel electrophoresis (PAGE) in fractions containing PrP 27-30 (3) have not been confirmed (36). Attempts to renature scrapie infectivity from guanidinium (Gdn) thiocyanate or urea were unsuccessful (36), but one group of investigators reported re-

* Corresponding author. Mailing address: Institut für Physikalische Biologie und Biologisch-Medizinisches Forschungszentrum, Heinrich-Heine-Universität Düsseldorf, 40225 Düsseldorf, Germany.

naturation of $PrP^{Sc}$ from 3 M Gdn-HCl on the basis of the restoration of resistance to proteinase K (17). Subsequent investigations failed to confirm this report of renaturation (13).

To identify conditions for solubilization of PrP 27-30, we examined a variety of ionic and nonionic detergents under conditions that were likely to retain scrapie prion infectivity. Sonication of purified prion rods in the presence of 0.2 to 0.3% SDS produced a soluble fraction that did not sediment during centrifugation at 100,000 × *g* for 1 h. This soluble fraction had a high α-helical content and relatively low β-sheet content compared with the amyloid polymers composed of PrP 27-30, and it contained spherical particles with an observed sedimentation coefficient of 6S and a diameter of ~10 nm. The spheres were composed of four to six PrP 27-30 molecules; they contained little, if any, scrapie infectivity. While our studies did not yield infectious preparations of soluble prions, they did provide fractions of PrP 27-30 oligomers which could be characterized with respect to aggregation, proteinase K resistance, and conformation.

TABLE 1. Efficiency of solubilization of PrP 27-30 by sonication in buffer A containing various detergents[a]

| Detergent in sonication buffer[b] | Level in supernatant | | |
|---|---|---|---|
| | PrP content (%) | Infectivity (%) | Log $ID_{50}$/ml |
| None | 1–2 | 2 | 6.4 |
| SDS (0.5–10%) | 20–30 | 8–50[c] | 7.4–8.4[c] |
| Sarkosyl (2%) | 20 | 50 | 9.1 |
| Zwittergent 3-12 (1–3%) | 10 | 2 | 7.2–7.6 |
| LDAO (1%) | 5 | <0.1 | 4.9 |
| Thesit (3%) | 10 | 7 | 7.4 |
| Dodecylmaltoside (3%) | 10 | 6 | 7.6 |
| DLPC | 1–2 | 4 | 7.1 |

[a] PrP 27-30 content was determined with serial dilutions by Western blotting, and infectivity was determined by bioassays in Syrian hamsters. After solubilization centrifugation according to the total supernatant protocol, the PrP 27-30 content and the infectivities of the supernatant and pellet were added; the percentage of the soluble fraction is listed.

[b] LDAO, lauryldimethylamineoxide; DLPC, detergent-lipid-protein complex.

[c] Not related to the SDS concentration in a monotonic way.

## MATERIALS AND METHODS

**Chemicals and enzymes.** HFIP and acetonitrile were of spectroscopic grade from Aldrich (Milwaukee, Wis.). All other chemicals and solvents from commercial sources were of reagent grade. Lipids were from Avanti Polar Lipids (Alabaster, Ala.). Dodecylmaltoside (dodecyl-β-D-maltopyranoside), lauryldimethylamineoxide, and thesit were kindly provided by W. Welte (Freiburg, Germany); the other detergents were from Calbiochem (San Diego, Calif.). Benzonase and proteinase K were from Merck (Darmstadt, Germany).

**Purification of PrP 27-30 and bioassays.** PrP 27-30 was purified from the brains of scrapie-infected Syrian hamsters (Lak:LVG; Charles River Laboratories) as described previously (38). The final purification step was either a sucrose gradient centrifugation or an ultrafiltration in which proteins of less than 300 kDa were removed and PrP was obtained in the retentate (10). Prions from both sources gave similar results.

Bioassays of scrapie prions were performed in Syrian hamsters by an incubation time interval procedure (35). The same correlation between inoculated dose and incubation time was found for homogenates, purified prion rods from sucrose gradient centrifugation, and detergent-lipid-protein complexes, indicating that a variety of chemical treatments and fractionation procedures did not alter the relationship between inoculated dose and incubation time.

**Sonication and differential centrifugation.** Sonication was carried out in a biosafety hood with a cup horn sonicator (Branson) at 40 W for 5 min at temperatures not exceeding 17°C unless otherwise stated. The sample was contained in a screw-cap Pyrex tube (1-cm diameter, 8 cm long) immersed 2 cm into the water bath of the sonicator and held at its top by a clamp. Thermostating of the sonication bath was established by a heat exchanger inside the hood and a thermostat (Haake) outside the hood. After sonication, the sample was centrifuged in a 1.5-ml Eppendorf tube (Beckman Instruments, Palo Alto, Calif.) in a TL-100 ultracentrifuge (Beckman Instruments). Sonication carried out in 440 μl of buffer A (20 mM morpholinepropanesulfonic acid [MOPS], 20 mM Tris [pH 7.2]) or buffer B (10 mM sodium phosphate [pH 7.0]) was followed by centrifugation in thick-wall polycarbonate tubes in a TLS-55 swinging-bucket rotor at 100,000 × *g* for 115 min at 4°C, and a 220-μl supernatant was collected from immediately below the meniscus. In this report, the procedure is referred to as the soluble fraction protocol. In another series of experiments, sonication was carried out in 250 μl of buffer, and either the whole sample was loaded onto the sucrose gradient or the supernatant of 220 to 230 μl was separated from the pellet by careful pipetting after centrifugation using a fixed-angle rotor TLA-100.3 at 60,000 × *g* or 100,000 × *g* for 1 h at 4°C. Experiments in which the entire supernatant including the meniscus was collected are referred to as the total supernatant protocol.

**Sucrose gradient centrifugation.** The sucrose gradients were preformed stepwise with 5, 12.5, and 20% sucrose in 10 mM sodium phosphate buffer (pH 7) in 4-ml polyallomer tubes, with an effective column height of ~53 mm. In some experiments, 0.2% SDS was added to the sucrose. A 200-ml aliquot of the supernatant from the solubilization centrifugation was loaded onto the gradient, and centrifugation was performed in an SW60 rotor at 60,000 rpm for 5.5 h at 4°C. It was estimated that the largest particles in the supernatant from the solubilization centrifugation (~25S) would just reach the bottom of the gradient under these conditions. Fractions were collected from either the top or the bottom of the tubes.

**PrP analysis.** One volume of loading buffer was added to the protein sample, boiled for 5 min, and analyzed by SDS-PAGE (12% acrylamide) (18). Proteins were transferred onto an Immobilon P membrane (Millipore) (50); the membrane was blocked for 1 h with 5% nonfat dry milk in TBST buffer (10 mM Tris-HCl [pH 8.0], 0.15 M NaCl, 0.01% Tween 20) and subsequently incubated with anti-PrP monoclonal antibody 3F4 (ascites fluid was 1:5,000) (14) in TBST for 1 h at room temperature and then with alkaline phosphatase-conjugated secondary antibody (Promega) for 30 min at room temperature (2). Immunoreactive proteins were stained with 5-bromo-4-chloro-3-indolylphosphate (BCIP) and nitroblue tetrazolium. In most cases, PrP was determined from dot blots visualized with an enhanced chemiluminescence system (ECL kit RPV 2108; Amersham) and scanned with a densitometer.

Samples were incubated with proteinase K at 50 μg/ml at 37°C for 1 h; in some experiments, 10 μg/ml at 37°C for times between 1 and 30 min was used. The lower concentration was used to study samples exhibiting partial resistance. The digestions were terminated by the addition of phenylmethylsulfonyl fluoride at a final concentration of 7.5 mM.

**CD.** Circular dichroism (CD) spectra were recorded with a Jasco model 720 spectropolarimeter, using 1- or 5-mm-path-length cylindrical cells at room temperature. All measurements were carried out in buffer B containing 0.2% SDS, which allowed readings to be taken down to 190 nm; data could not be recorded below this wavelength because of excessive absorption by the buffer. Typically 20 to 50 spectra were recorded over the spectral range of 190 to 260 nm at a scan speed of 50 nm/min. A blank spectrum for the cuvette and buffer was recorded and subtracted from each spectrum; the largest amplitude of the blank was <5% relative to the spectra of the samples. Signal averaging allowed satisfactory CD spectra to be obtained with PrP 27-30 concentrations down to ~10 μg/ml. For those readings taken in the presence of acetonitrile, this reagent was added to the buffer after sonication. Quantitative secondary structure assignments were carried out with a computer program kindly provided by W. Curtis Johnson, University of Oregon (12). The accuracy of these assignments may be limited by truncation of the data at 190 nm.

**Electron microscopy.** The samples were adsorbed for about 20 s onto glow-discharged, carbon-coated grids. Excess material and sucrose were washed away with three drops each of 0.1 and 0.01 M ammonium acetate. The grids were then stained with 2% uranyl acetate and viewed in a JEOL 100CX II electron microscope at 80 kV. Negatively stained catalase crystals were used for calibration. The diameter of the particles was measured parallel to one side of each print, independent of the orientation of the particles.

## RESULTS

**Dispersion of prion rods.** Sonication of prion rods (~300 μg of PrP 27-30 per ml) was performed in buffer A with a variety of detergents. After sonication, the samples were centrifuged in a fixed-angle rotor at 60,000 × *g* at 4°C for 1 h, and the supernatant was sampled according to the total supernatant protocol. The effectiveness of the detergent was evaluated on the basis of the fraction of the PrP 27-30 and the scrapie infectivity remaining in the supernatant, as determined by Western blots and bioassays (Table 1). The most effective detergents were SDS and Sarkosyl, both of which liberated 20 to 30% of PrP 27-30 and prion infectivity in the supernatant. SDS concentrations of 0.5% up to 10% were investigated, but the extent of solubilization appeared to be independent of SDS concentration, probably because all concentrations were above

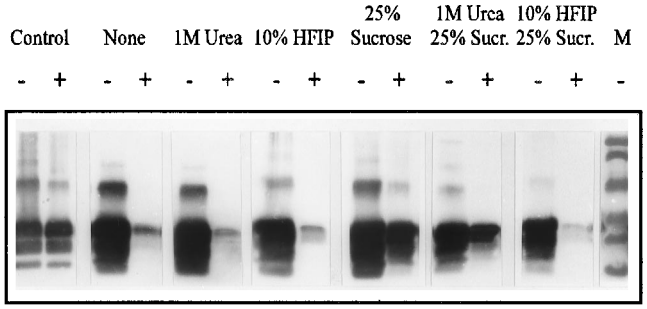


FIG. 1. Western blot of PrP 27-30 in the supernatant prepared according to the total supernatant protocol. Samples designated '+' were digested with 50 μg of proteinase K per ml at 37°C for 1 h. All sonication buffers contained buffer A and 0.3% SDS. The pellet after sonication without additives and centrifugation served as a control. The additives to the sonication buffer are indicated for the different samples. Sucr., sucrose. Molecular mass markers (M) are proteins of 106, 80, 49.5, 32.5, 27.5, and 18.5 kDa.

the critical micelle concentration (~0.24%). The finding that SDS and Sarkosyl did not inactivate scrapie infectivity at low concentrations is in agreement with earlier findings (37).

In additional studies, centrifugation was increased from 60,000 × *g* to 100,000 × *g* while other parameters were held constant. The presence of protein in the supernatant after centrifugation at 100,000 × *g* for at least 1 h with an 8-mm column height is an accepted criterion for solubilization (11). Proteins or protein aggregates with a sedimentation coefficient of larger than 25S, corresponding to an $M_r$ of $>10^6$, would sediment into the pellet during a 1-h centrifugation with 8-mm column height. The effect of SDS concentrations was reinvestigated by applying concentrations of 0.05 to 1%. Maximum solubilization was achieved at ~0.3% SDS, which is near the critical micelle concentration. For all subsequent experiments, the sonication was carried out with 0.2 or 0.3% SDS.

Time and temperature of sonication were varied between 5 and 30 min and 17 and 37°C, respectively. The fractions of PrP recovered in the supernatant according to the total supernatant protocol were similar for all of the conditions examined. In an attempt to minimize denaturation, we used 5 min of sonication starting at 7°C, with the temperature increasing to no more than 17°C. It is noteworthy that prolonged sonication of Syrian hamster brain homogenates did not reduce infectivity (41).

Chaotropic agents known to denature PrP 27-30 and destroy infectivity were used at low concentrations, e.g., 1 M urea or 0.5 M Gdn-HCl (36, 37). The effect of HFIP on prion infectivity was evaluated at a concentration of 10% (vol/vol). Sucrose was also added up to 25% (wt/vol), either alone or in combination with the other reagents. After sonication in 0.3% SDS, the fraction of PrP 27-30 remaining in the supernatant was considerably more sensitive to digestion with proteinase K than that in the prion rods found in the pellet (Fig. 1). Bioassays of these digested supernatant fractions showed reductions in prion titers by factors 5, 16, 3, 50, and 5 in five independent experiments. While such changes are not significant, there was always a small reduction of titer. In contrast, HFIP diminished the infectivity drastically; other reagents did not appear to be promising, and so further studies were not performed. The apparent protection of sucrose against proteinase K digestion is due to its influence of viscosity and density on the 100,000 × *g* centrifugation. Thus, in all subsequent experiments, the prion sample for sonication contained only buffer and 0.2 or 0.3% SDS.

**Sucrose gradient centrifugation analysis.** To characterize the prions in the supernatant after sonication in 0.2% SDS, we designed a protocol using sucrose gradient centrifugation to determine whether PrP 27-30 and infectivity cosedimented. To minimize contamination of the supernatant fraction by any particles floating in the meniscus or particles loosely adherent to the pellet, centrifugation of the SDS-sonicated prion rods was performed in a swinging-bucket rotor, and only 50% of the supernatant was collected with a pipette from the upper portion of the liquid column. This is the soluble fraction protocol. To distribute the supernatant over the entire sucrose gradient (5 to 20%) with a 53-mm column height, a value of $6.4 \times 10^{11}$ $rad^2/s$ for $\int\omega^2 dt$ (60,000 rpm, 5.5 h in a Ti60 rotor) was chosen.

The gradients were preformed with either no detergent or 0.2% SDS to test for reaggregation in the absence of SDS. Gradients were fractionated from either the top or the bottom to assess possible artifacts. Profiles for PrP 27-30 content and scrapie infectivity in the presence or absence of SDS in the sucrose gradients were similar; values are the means from four or five independent experiments (Fig. 2). The majority of PrP 27-30 was found in fractions 2 to 5 and sedimented as a symmetrical peak of ~6S, but only ~0.02% of the infectivity was recovered in these fractions. It is noteworthy that the supernatant collected by the soluble fraction protocol contained only 6% of the total infectivity, of which 50% was loaded onto the gradient (Table 2). Because the specific infectivity in fractions 2 to 5 was nearly 3 orders of magnitude lower than that of the prion rods, we conclude that soluble PrP 27-30 prepared under these conditions is devoid of prion infectivity.

To explore the reasons for the low recovery of the infectivity in the supernatant fractions (Table 2) loaded onto the gradients in Fig. 2 compared with the nearly 50% infectivity in the supernatant in the initial SDS sonication experiments (Table 1), prion rods were sonicated in 0.2% SDS and loaded directly onto the sucrose gradient without prefractionation by differential centrifugation. Again, most of the PrP 27-30 was found in fractions 2 to 5 (Fig. 3), but some PrP 27-30 was also found in the meniscus fraction. Most notably, $\sim 10^7$ 50% infectious doses ($ID_{50}$) of prion infectivity per ml were found in the meniscus and the adjacent fraction as well as at the bottom of the gradient, in contrast to fractions 3 to 5, containing most of the PrP 27-30, in which prion titers were lower by nearly a factor of 1,000. When prion rods were sonicated in 0.2% SDS and separated into supernatant and pellet fractions according to the total supernatant protocol (Table 1 and Fig. 1), the sedimentation profiles of PrP 27-30 and prion infectivity were similar to those shown in Fig. 3 (data not shown).

The prions in the meniscus fractions would seem to be of either small size or low density. Since the supernatant fractions prepared with the soluble fraction protocol would have eliminated the prions of low density but not those of small size, we conclude that the absence of infectivity in the meniscus fraction in Fig. 2 indicates a low density population of prions. Most likely the low density of the prions is due to lipids and possibly detergents bound to PrP 27-30. The origin of the lipids has to be the prion rods.

**Ultrastructural analysis.** Fractions 2 to 5 of the sucrose gradients (Fig. 2 and 3) contained numerous spherical particles (Fig. 4A and B). Since these fractions contain only PrP 27-30 as judged by SDS-PAGE, and no particles other than spheres were found by electron microscopy, we conclude that the spheres are composed of PrP 27-30. Most of the spheres ranged from 8 to 12 nm in diameter; a substantial portion had diameters of ~10 nm (Fig. 4C). We were unable to identify any consistent substructure by using negative staining.

Since these particles were spherical, we estimated the mo-

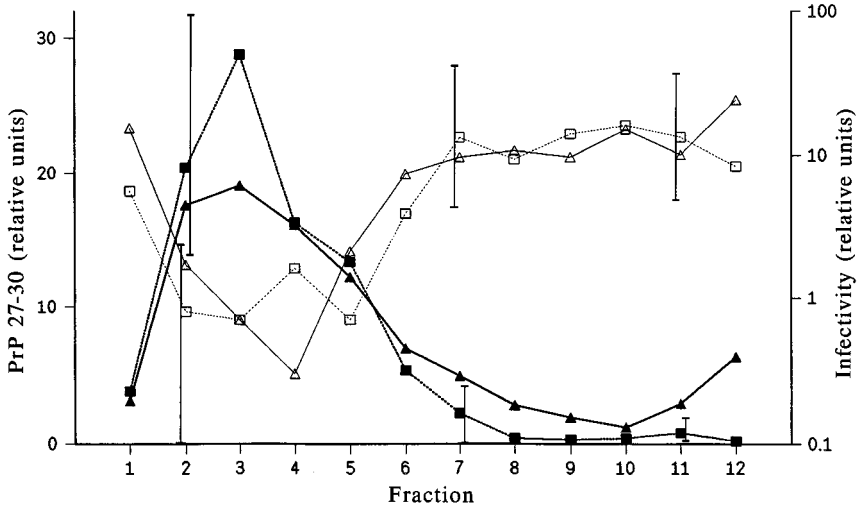


FIG. 2. Analysis by 5 to 20% sucrose gradient centrifugation of the supernatant prepared according to the soluble fraction protocol. The sedimentation profiles show PrP 27-30 (■) and infectivity (□) in the presence of 0.2% SDS and PrP 27-30 (▲) and infectivity (△) without SDS in the gradient. All values are the means of four (without SDS) or five (with SDS) independent experiments. Relative units are depicted (in percentages) for PrP 27-30 and infectivity; the sum of all fractions is set to 100%. A value of 100 for prion infectivity corresponds to values of $10^{5.2}$ to $10^{7.4}$ $ID_{50}$ in the different gradients (see Table 2). Error bars are defined by the highest and the lowest values; they are shown for three fractions only but are characteristic for all fractions. The low level of prion infectivity and possibly the adjacent PrP peak contribute to the large error bars in fraction 2.

lecular weight from the average sedimentation coefficient (~6S) determined from the position of the peak fraction. The partial specific volume ($v$) for a sedimenting particle was calculated according to the method of Durchschlag (6) to be 0.71 $cm^3\ g^{-1}$, on the basis of the following composition of PrP 27-30: 54% protein ($v$ = 0.71 $cm^3\ g^{-1}$), 18% carbohydrate ($v$ = 0.65 $cm^3\ g^{-1}$), 7% glycolipid anchor ($v$ = 0.59 $cm^3\ g^{-1}$), and 21% SDS, i.e., 0.4 g of SDS per g of protein ($v$ = 0.82 $cm^3\ g^{-1}$), determined as described by Tanford (47) and assuming hydration as 0.5 g of water per g of PrP 27-30 (the values for SDS binding and hydration being rough estimates only). Applying the standard method for evaluation of a spherical molecule of 6S (4), a molecular mass of 117 kDa was obtained, which corresponds to pentamer of PrP 27-30. Allowing for uncertainties in this calculation, we conclude that each of these spheres contains between four and six PrP 27-30 molecules. Although the 10-nm diameter is somewhat larger than expected for a globular aggregate of 117 kDa, errors in some of our estimates may account for this small discrepancy. On the other hand, the observed sedimentation values for PrP 27-30 and the spheres suggest that PrP 27-30 is unlikely to form particles other than the spheres visualized by electron microscopy.

The meniscus fraction in Fig. 3 containing substantial infectivity possessed a heterogeneous array of particles, many of which are vesicular and appeared to be composed largely of lipid (Fig. 5A); in addition, aggregates of small rods were found (Fig. 5B). The finding of rod fragments in the meniscus fractions implies that the density of these fragments is below 1.018 $g/cm^3$ (5% sucrose) and that they are associated with substantial amounts of lipid. The pellet fraction also contained rod fragments which survived the sonication procedure (data not shown). Whether the spheres contain small amounts of lipid or other compounds remains to be determined.

**Conformational transitions.** Conformational analyses were performed on the supernatant and the resuspended pellet fractions. After the supernatants were collected for sucrose gradient analysis by the soluble fraction protocol, the remaining supernatant fractions were collected and examined by CD spectroscopy. The pellet was resuspended in an equal volume of the same buffer. The supernatant exhibited a spectrum char-

TABLE 2. Reduction in levels of infectivity[a]

| Expt | Sample | Log $ID_{50}$ | | Recovery (%) |
|---|---|---|---|---|
| | | Mean | Range | |
| A | From the soluble fraction protocol | | | |
| | Pellet after solubilization centrifugation | 9.0 | 7.3–9.3 | 94 |
| | Supernatant after solubilization centrifugation | 7.8 | 6.1–8.7 | 6 |
| | Total infectivity recovered from sucrose gradient | 6.8 | 5.2–7.4 | 0.6 |
| B | From the total supernatant protocol | | | |
| | Pellet after solubilization centrifugation | 7.6 | | 72 |
| | Supernatant after solubilization centrifugation | 7.1 | | 28 |
| | Total infectivity recovered from sucrose gradient | 6.9 | | 15 |

[a] Prion rods were sonicated in 0.2% SDS and separated into pellet and supernatant after the solubilization centrifugation. The supernatant (soluble fraction protocol) was further loaded onto a sucrose gradient for size determination. For the calculation of recovery, the infectivities of the supernatant and pellet after solubilization centrifugation were added (100%); the corresponding percentages are listed. Mean values from experiment A are from 11 separate determinations; those from experiment B are from 2 determinations.

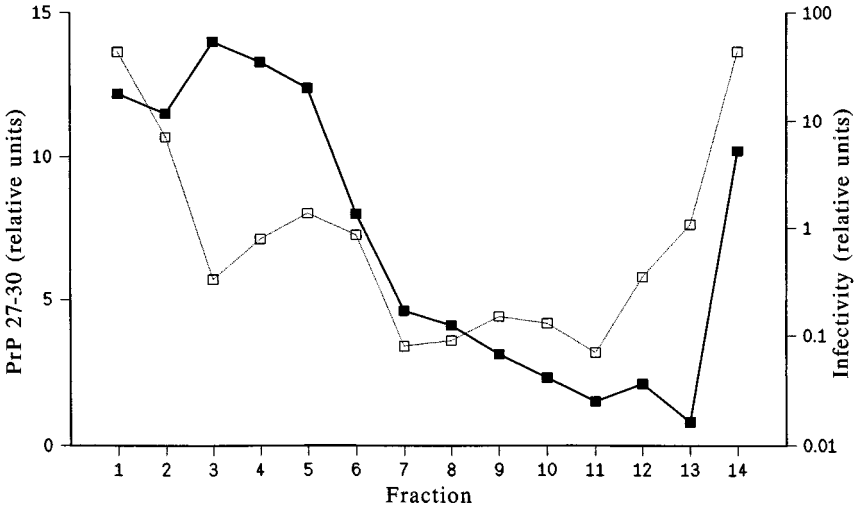


FIG. 3. Fractionation by 5 to 20% sucrose gradient centrifugation of the total sample after sonication in the presence of SDS. The sucrose gradient did not contain SDS. The sedimentation profiles show PrP 27-30 (■) and infectivity (□) as in Fig. 2, derived from the mean of two independent experiments. A value of 100 for prion infectivity corresponds to $10^{6.9}$ $ID_{50}$ (see Table 2).

acteristic of proteins with high α-helical content, whereas the pellet exhibited a high β-sheet content. These spectra were similar to those obtained on fractions prepared by using the total supernatant protocol; that is, the supernatant (Fig. 6A) showed minima at 208 and 222 nm, characteristic for α-helical structures. The pellet fraction gave a maximum at 195 nm and a minimum at 218 nm, values which are representative of β sheets. The spectrum of the supernatant showed no changes over a 24-h period, suggesting that the PrP 27-30 remained soluble over this time interval. In contrast, the ellipticity of the resuspended pellet decreased measurably over 1 h in accord with the insolubility of the rods. When the prion rods were sonicated for up to 1 h without SDS, the supernatant fraction gave a lower ellipticity spectrum with a characteristic β-sheet signal, suggesting that the conformation of PrP 27-30 in the broken rods was unaltered by sonication.

Since acetonitrile is known to induce β sheets in peptides (24, 26, 48), we studied the influence of acetonitrile on the spectrum of the supernatant fraction. Increasing the acetonitrile concentration from 0 to 50% in increments of 10% induced a progressive shift from α helix to β sheet (Fig. 6B). The proportions of α-helix and β-sheet structures determined from the CD spectra were tabulated (Table 3). The α-helix content of the supernatant fractions ranged from 40 to 60%; this variation may be due to inconstancies in the SDS sonication procedure as well as the protocol used to separate the supernatant from the pellet after centrifugation in a fixed-angle rotor. The addition of 10 or 20% acetonitrile effected a small reduction in the α-helix content and a concomitant increase in β-sheet content; 30% acetonitrile produced approximately equal amounts of α helix and β sheet. The spectra of the resuspended pellet resembled that of the supernatant to which 30% acetonitrile had been added (Table 3). Concentration of 40 or 50% acetonitrile seemed to denature PrP 27-30. The addition of 25 to 50% acetonitrile to the supernatant precipitated PrP 27-30 after exposure overnight, as assessed by centrifugation at 100,000 × *g*.

Since infectious prion rods containing PrP 27-30 are rich in β sheet, we investigated whether the increase in β sheet due to acetonitrile was accompanied by an increase in infectivity. Addition of 10 to 20% acetonitrile had no effect on prion infectivity, while 30% acetonitrile reduced infectivity ~75%. Addition of 40 to 50% acetonitrile diminished prion titers by a factor of $10^3$ to $10^4$. Thus, the conformational change induced by acetonitrile is not equivalent to that which occurs during the formation of $PrP^{Sc}$. It seems likely that acetonitrile at concentrations above 30% denatures $PrP^{Sc}$.

Electron microscopy was also used to monitor the effect of acetonitrile on the supernatant following SDS sonication and centrifugation. No rods were found in the presence of 25% acetonitrile, but aggregates could assemble from soluble PrP 27-30 (Fig. 5C).

Fractions containing PrP 27-30 after sonication in 0.2% SDS and sucrose gradient centrifugation (Fig. 3) as well as after addition of 30% acetonitrile were examined for proteinase K resistance. The majority of the PrP 27-30 in the meniscus fraction was digested within the first minute, whereas the remaining PrP 27-30 was stable for 30 min (Fig. 7A). This behavior may reflect the array of structures found by electron microscopy (Fig. 5A and B), with aggregates of rods being responsible for the residual proteinase K resistance. In contrast, the soluble PrP 27-30 from the peak fractions was digested nearly completely within the first minute (Fig. 7B). The pellet obtained after SDS sonication of prion rods followed by centrifugation in a fixed-angle rotor exhibited substantial proteinase K resistance (Fig. 7C). When the peak fraction was treated with 30% acetonitrile and precipitated PrP 27-30 was recovered by a 100,000 × *g* centrifugation, measurable but modest proteinase K resistance was found (Fig. 7D).

## DISCUSSION

Considerable evidence supports the hypothesis that a conformational change in PrP underlies both the propagation of prions and the pathogenesis of prion diseases (5, 29). This proposal emerges from spectroscopic studies comparing $PrP^{C}$ in a purified sample with $PrP^{Sc}$ in another highly enriched fraction. Transgenetic studies argue persuasively that $PrP^{C}$ and $PrP^{Sc}$ interact during the formation of nascent $PrP^{Sc}$ (39, 49). The investigations reported here address this issue from the perspective of starting with a uniform sample of prions and modifying the structure of PrP 27-30 under relatively gentle

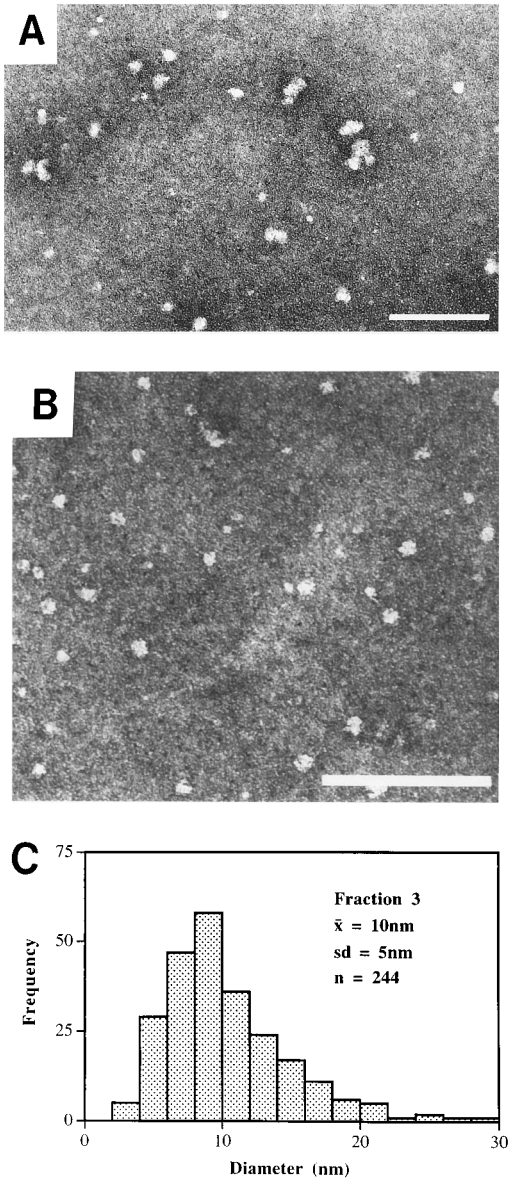


FIG. 4. Electron microscopy of the peak fractions collected from sucrose gradients after centrifugation. (A) Fraction 3 from gradient shown in Fig. 2. (B) Fraction 3 from gradient shown in Fig. 3. Bars = 100 nm. (C) Size distribution of the spherical particles in panel A.

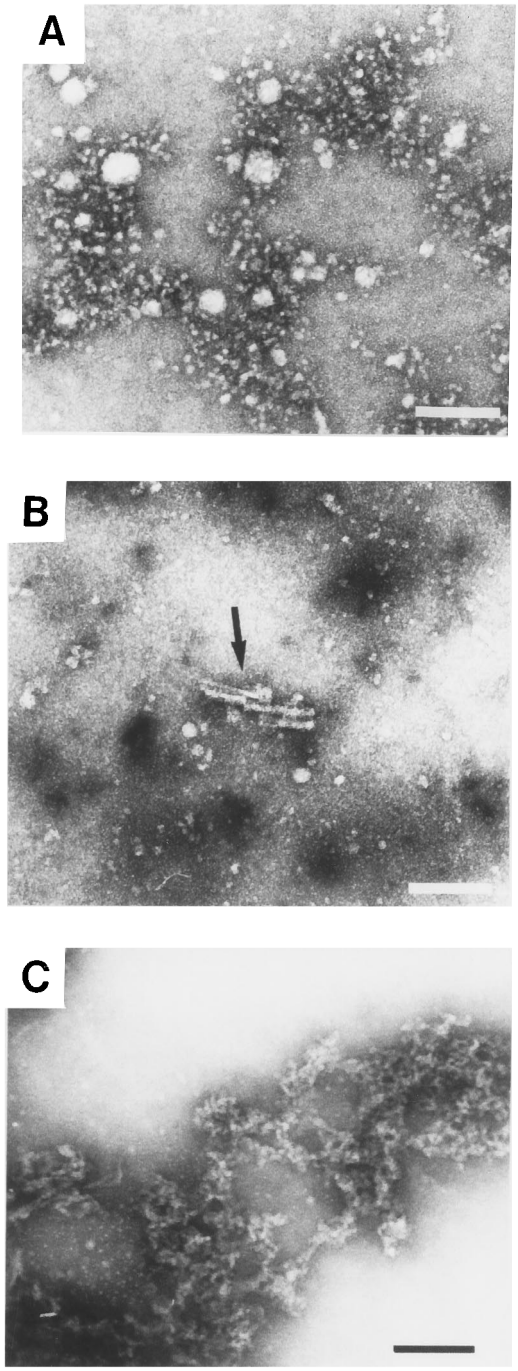


FIG. 5. Electron micrographs of fractions containing PrP 27-30. (A and B) Two samples of the meniscus fraction from the sucrose gradient illustrated in Fig. 3. The arrow points to residual rod fragments. (C) The supernatant fraction was prepared according to the total supernatant protocol, 25% acetonitrile was added, and the precipitate was collected by centrifugation. The resuspended pellet is shown. Bars = 100 nm.

conditions. Sonication in 0.2% SDS transformed prion rods into a variety of multimeric structures which were characterized by solubility, conformation, proteinase K resistance, and infectivity.

**Fractionation of prion rods.** After sonication of prion rods in the presence of 0.2% SDS, ~25% of the PrP 27-30 was found in the supernatant after centrifugation at 100,000 × *g* for 1 h. The pellet contained the majority of PrP 27-30, consisting of prion rods which withstood the SDS-sonication procedure, but the rods were smaller as measured by electron microscopy (data not shown). The CD spectrum of this pellet fraction showed a more pronounced β-sheet signal than that of prion rods subjected to sonication in the absence of SDS (Fig. 6A).

Disruption of prion rods by sonication in the presence of 0.2 to 0.3% SDS suggested that scrapie infectivity was preserved under these conditions (Table 1), but fractionation by sucrose gradient centrifugation gave results which appeared inconsistent with the initial bioassay data (Fig. 2). This discrepancy seems to be due to the use of different protocols; there were high levels of infectivity in the total supernatant but low levels in the soluble fraction, using slightly different protocols for recovery of the supernatant fractions. Sonication in the pres-

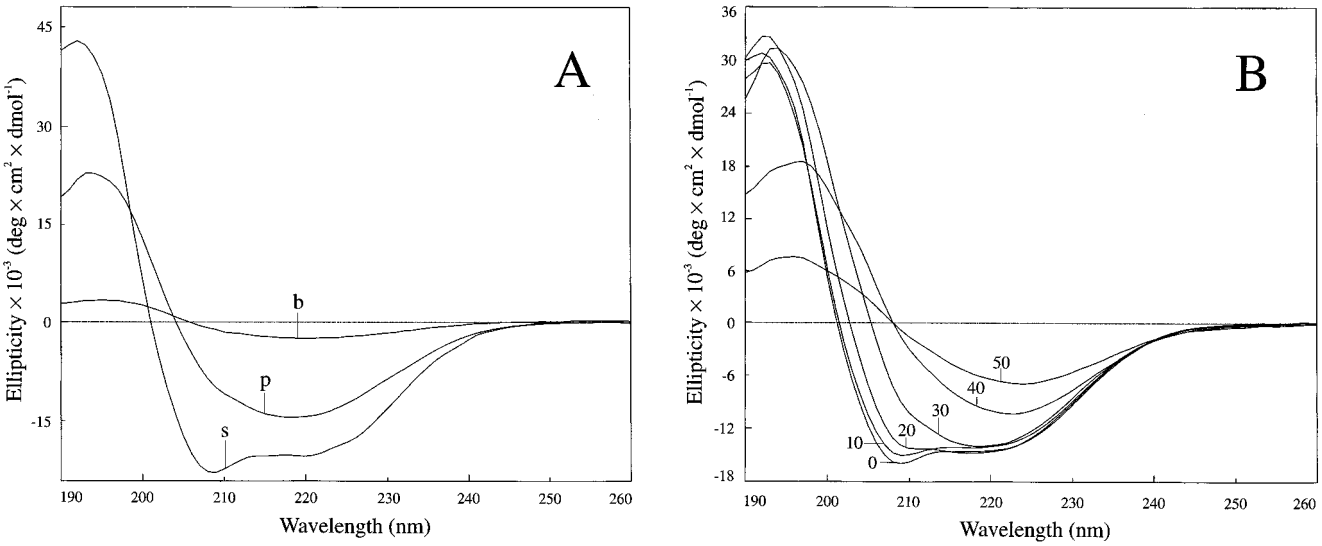


FIG. 6. CD spectra. (A) Supernatant (s) and pellet (p) were prepared according to the total supernatant protocol in 10 mM phosphate buffer (pH 7.0) containing 0.2% SDS; broken rods (b) were obtained by sonication for 1 h in the absence of SDS and without centrifugation. (B) Supernatant after addition of 0 to 50% (in steps of 10%) acetonitrile. Ellipticities were calibrated according to an amino acid analysis of the sample and were corrected for dilution with acetonitrile.

ence of SDS generated a lipid-rich fraction with a low buoyant density and substantial levels of scrapie infectivity (Fig. 3) that was included in the total supernatant but was excluded from the soluble fraction. The lipid-rich, infectious prions were identified in the meniscus fraction of sucrose gradients when the total supernatant procedure was used to generate the sample loaded onto the gradient (Fig. 3). It should be emphasized that the lipids or other compounds which are responsible for the low density of the prions were not added during sonication but are constituents of the prion rods. A heterogeneous array of particles including spheres of different sizes, aggregates of spheres, and even small prion rod-like structures, were found by electron microscopy of lipid-rich fractions (Fig. 5). Also, a portion of the PrP 27-30 (Fig. 7) as well as the prion infectivity was destroyed by proteinase K digestion, whereas residual PrP 27-30 and infectivity resisted limited digestion. Possibly the rod-shaped structures in the lipid-rich fraction represent a proteinase K-resistant subpopulation of PrP 27-30 molecules that are associated with prion infectivity. Our results suggesting that lipids may stabilize the conformation of PrP 27-30 and thus preserve prion infectivity are consistent with earlier studies in which delipidation led to inactivation of scrapie infectivity (22). In fact, some investigators argue that the bovine spongiform encephalopathy epidemic resulted from inadequate delipidation of the protein-rich greaves which was processed into meat and bone meal (MBM). In contrast to earlier rendering procedures of animal offals using organic solvent extraction, which produced MBM containing ~1% fat and apparently devoid of prions, more recent protocols omitting solvent extraction produced MBM containing ~14% fat in which sheep prions and later those from cattle seemed to have survived (51).

**Spherical particles composed of PrP 27-30.** By sedimentation analysis and electron microscopy, the spherical particles appear to contain four to six PrP 27-30 molecules. The PrP 27-30 molecules that form these spheres resemble $PrP^C$ and denatured PrP 27-30 in several aspects: PrP 27-30 is soluble, it is sensitive to proteinase K digestion, it has a high α-helical and low β-sheet content, and it is not associated with scrapie infectivity (9, 29, 42). Of note, PrP 27-30 denatured by exposure to 3 M NaOH, boiling in 2% SDS, or 6 M Gdn does not form spherical particles to our knowledge (25, 42). Although it seems unlikely that $PrP^C$ forms spherical particles of four to six molecules when it is tethered to the plasma membrane by its glycerolphosphatidylinositol anchor, it is likely that $PrP^C$ aggregates into micelles when it is solubilized by exposure to nondenaturing detergents. Indeed, the formation of spheres by PrP 27-30 seems to be facilitated by SDS; whether PrP 27-30

TABLE 3. Effects of acetonitrile on the infectivity of the supernatant after solubilization centrifugation and on the secondary structure as determined by CD spectroscopy[a]

| Sample | Acetonitrile (%) | Log $ID_{50}$/ml | Infectivity (%) | Secondary structure (%) | | | |
|---|---|---|---|---|---|---|---|
| | | | | α helix | β sheet | Turns | Other |
| Pellet fraction | 0 | 9.6 | 83 | 29 | 31 | 10 | 30 |
| Supernatant fraction | 0 | 8.9 | 17 | 61 | 5 | 16 | 18 |
| | 10 | 9.1 | 26 | 57 | 9 | 15 | 19 |
| | 20 | 8.9 | 17 | 53 | 18 | 9 | 20 |
| | 30 | 8.4 | 5 | 37 | 33 | 5 | 25 |
| | 40 | 5.9 | 0.02 | 26 | 36 | 6 | 32 |
| | 50 | 5.0 | 0.002 | 22 | 29 | 13 | 36 |

[a] The total infectivity of pellet and supernatant (100%) after solubilization centrifugation was 9.7 log $ID_{50}$/ml.

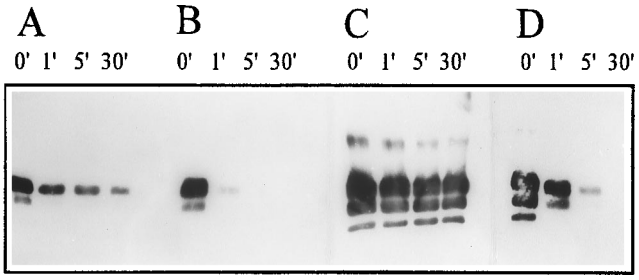


FIG. 7. Western blots showing variable proteinase K resistance of PrP 27-30 fractions from solubilization experiments. (A) PrP 27-30 from the meniscus of the gradient in Fig. 3. (B) PrP 27-30 from fraction 3 of the gradient in Fig. 3. (C) PrP 27-30 in the pellet from the soluble fraction protocol and (D) PrP 27-30 from fraction 3 of the gradient in Fig. 4 after addition of 30% acetonitrile. The incubation times were 0, 1, 5, and 30 min at 37°C at a final concentration of 10 μg of proteinase K per ml.

molecules in these spheres aggregate through their glycerol-phosphatidylinositol anchors or interact through other domains in the molecule remains to be established.

The spheres of PrP 27-30 reported here resemble morphologically those generated by sonication of prion rods in the absence of SDS, a nonsedimenting fraction contained spherical particles of 8- to 20-nm diameter as judged by electron microscopy, but the yield was so low that the particles could not be characterized in more detail (20). Some investigators attempted to determine the size of infectious prions by using sucrose gradient centrifugation after extraction of Creutzfeldt-Jakob disease-infected mouse brain preparations with Sarkosyl and sonication (45). A noninfectious peak of ~7S containing PrP was found, which was interpreted as composed of "monomeric or dimeric" PrP molecules. From these findings, the authors concluded that PrP can be separated from infectivity and therefore cannot be the major or essential component of the infectious prion. It seems likely that the 7S PrP peak in those studies is composed of the same spherical oligomers of PrP 27-30 reported here. Other studies described spherical particles with an average diameter of 12 nm in brain homogenates from scrapie-infected Syrian hamsters but not from uninfected controls (27). Similar spheres have also been found in homogenates prepared from the brains of patients who died of Creutzfeldt-Jakob disease (28). The investigators have referred to the spherical particles as "virus-like" and suggest they are the agents of the disease that induce the formation of $PrP^{Sc}$ as a secondary effect. Considering that the spheres in the brain homogenates were seen after digestion with proteinase K in the presence of detergent which produces PrP 27-30, it seems likely that these 12-nm spheres are the same as the spherical oligomers of PrP 27-30 reported here.

**Conformational transitions of PrP 27-30.** The high α-helical content of PrP 27-30 in the spheres was converted into β sheet by exposure to 25 to 30% acetonitrile. Under these conditions, the PrP 27-30 aggregated into insoluble, irregular polymers (Fig. 7) and exhibited partial resistance to digestion by proteinase K, which presumably is a consequence of the aggregation. It seems likely that aggregation and insolubility of the acetonitrile-treated spheres resulted from the β-sheet conformation which PrP 27-30 acquired. These aggregates of PrP 27-30 were clearly distinct from the prion rods morphologically and did not possess scrapie infectivity as measured by bioassay in hamsters.

Evidence for intermediate, partially folded states of $PrP^{Sc}$ and PrP 27-30 have been obtained by exposure of these proteins to 2 M Gdn-HCl or to pH <2, using CD spectroscopy (43). Whether these "molten globules" are equivalent to the structure of PrP 27-30 in the spherical particles reported here remains to be established. It is noteworthy that some investigators have reported reversible denaturation of $PrP^{Sc}$ with 3 M Gdn-HCl on the basis of the restoration of resistance to proteinase K (17). In studies performed by some of us, no evidence for renaturation of $PrP^{Sc}$ under these conditions could be obtained; it seems likely that some of the $PrP^{Sc}$ was denatured in 3 M Gdn-HCl and formed a proteinase K-sensitive fraction, while the remainder was not denatured, persisted as insoluble aggregates, and continued to be resistant to protease digestion (13). This interpretation is in accord with bioassays performed on prion fractions exposed to Gdn at various concentrations followed by dilution; no restoration of infectivity could be demonstrated as reported here for the spheres containing PrP 27-30 (36). The relatively uniform size of the spheres suggests that the PrP 27-30 molecules comprising them possess a unique metastable conformation which produces this distinct quaternary structure. Whether conditions which renature the PrP 27-30 in the spheres and restore scrapie infectivity can be identified remains unknown, but is certainly worthy of further investigation.

## ACKNOWLEDGMENTS

This work was supported by research grants from the National Institutes of Health (NS22786), the Ministerium für Wissenschaft und Forschung of NRW, and the Bundesministerium für Forschung und Technologie.

## REFERENCES

1. **Alper, T., D. A. Haig, and M. C. Clarke.** 1966. The exceptionally small size of the scrapie agent. Biochem. Biophys. Res. Commun. **22:**278–284.
2. **Blake, M., K. H. Johnson, G. J. Russel-Jones, and E. Gotschlich.** 1984. A rapid, sensitive method for detection of alkaline phosphatase-conjugated anti-antibody on Western blots. Anal. Biochem. **136:**175–179.
3. **Brown, P., P. P. Liberski, A. Wolff, and D. C. Gajdusek.** 1990. Conservation of infectivity in purified fibrillary extracts of scrapie-infected hamster brain after sequential enzymatic digestion or polyacrylamide gel electrophoresis. Proc. Natl. Acad. Sci. USA **87:**7240–7244.
4. **Cantor, C. R., and P. R. Schimmel.** 1980. Biophysical chemistry. W. H. Freeman and Co., San Francisco.
5. **Cohen, F. E., K.-M. Pan, Z. Huang, M. Baldwin, R. J. Fletterick, and S. B. Prusiner.** 1994. Structural clues to prion replication. Science **264:**530–531.
6. **Durchschlag, H.** 1986. Specific volumes of biological macromolecules and some other molecules of biological interest, p. 45–128. *In* H.-J. Hinz (ed.), Thermodynamic data for biochemistry and biotechnology. Springer-Verlag, Berlin.
7. **Gabizon, R., M. P. McKinley, and S. B. Prusiner.** 1987. Purified prion proteins and scrapie infectivity copartition into liposomes. Proc. Natl. Acad. Sci. USA **84:**4017–4021.
8. **Gajdusek, D. C.** 1977. Unconventional viruses and the origin and disappearance of kuru. Science **197:**943–960.
9. **Gasset, M., M. A. Baldwin, R. J. Fletterick, and S. B. Prusiner.** 1993. Perturbation of the secondary structure of the scrapie prion protein under conditions associated with changes in infectivity. Proc. Natl. Acad. Sci. USA **90:**1–5.
10. **Hecker, R., A. Taraboulos, M. Scott, K.-M. Pan, M. Torchia, K. Jendroska, S. J. DeArmond, and S. B. Prusiner.** 1992. Replication of distinct prion isolates is region specific in brains of transgenic mice and hamsters. Genes Dev. **6:**1213–1228.
11. **Hjelmeland, L. M., and A. Chrambach.** 1984. Solubilization of functional membrane proteins. Methods Enzymol. **104:**305–318.
12. **Johnson, W. C., Jr.** 1990. Protein secondary structure and circular dichroism: a practical guide. Proteins **7:**205–214.
13. **Kaneko, K., D. Peretz, K.-M. Pan, T. Blochberger, R. Gabizon, O. H. Griffith, F. E. Cohen, M. A. Baldwin, and S. B. Prusiner.** 1995. Prion protein (PrP) synthetic peptides induce cellular PrP to acquire properties of the scrapie isoform. Proc. Natl. Acad. Sci. USA **92:**11160–11164.
14. **Kascsak, R. J., R. Rubenstein, P. A. Merz, M. Tonna-DeMasi, R. Fersko, R. I. Carp, H. M. Wisniewski, and H. Diringer.** 1987. Mouse polyclonal and monoclonal antibody to scrapie-associated fibril proteins. J. Virol. **61:**3688–3693.
15. **Kellings, K., N. Meyer, C. Mirenda, S. B. Prusiner, and D. Riesner.** 1992.

Further analysis of nucleic acids in purified scrapie prion preparations by improved return refocussing gel electrophoresis (RRGE). J. Gen. Virol. **73:**1025–1029.
16. **Kimberlin, R. H., G. C. Millson, and G. D. Hunter.** 1971. An experimental examination of the scrapie agent in cell membrane mixtures. III. Studies of the operational size. J. Comp. Pathol. **81:**383–391.
17. **Kocisko, D. A., J. H. Come, S. A. Priola, B. Chesebro, G. J. Raymond, P. T. Lansbury, Jr., and B. Caughey.** 1994. Cell-free formation of protease-resistant prion protein. Nature (London) **370:**471–474.
18. **Laemmli, U. K.** 1970. Cleavage of structural proteins during the assembly of the head of bacteriophage T4. Nature (London) **227:**680–685.
19. **Malone, T. G., R. F. Marsh, R. P. Hanson, and J. S. Semancik.** 1978. Membrane-free scrapie activity. J. Virol. **25:**933–935.
20. **McKinley, M. P., M. B. Braunfeld, C. G. Bellinger, and S. B. Prusiner.** 1986. Molecular characteristics of prion rods purified from scrapie-infected hamster brains. J. Infect. Dis. **154:**110–120.
21. **Meyer, R. K., M. P. McKinley, K. A. Bowman, M. B. Braunfeld, R. A. Barry, and S. B. Prusiner.** 1986. Separation and properties of cellular and scrapie prion proteins. Proc. Natl. Acad. Sci. USA **83:**2310–2314.
22. **Millson, G. C., G. D. Hunter, and R. H. Kimberlin.** 1976. The physicochemical nature of the scrapie agent, p. 243–266. *In* R. H. Kimberlin (ed.), Slow virus diseases of animals and man. American Elsevier, New York.
23. **Millson, G. C., and E. J. Manning.** 1979. The effect of selected detergents on scrapie infectivity, p. 409–424. *In* S. B. Prusiner and W. J. Hadlow (ed.), Slow transmissible diseases of the nervous system, vol. 2. Academic Press, New York.
24. **Nguyen, J., M. A. Baldwin, F. E. Cohen, and S. B. Prusiner.** 1995. Prion protein peptides induce α-helix to β-sheet conformational transitions. Biochemistry **34:**4186–4192.
25. **Oesch, B., M. Jensen, P. Nilsson, and J. Fogh.** 1994. Properties of the scrapie prion protein: quantitative analysis of protease resistance. Biochemistry **33:** 5926–5931.
26. **Otvos, L., Jr., G. I. Szendrei, V. M. Lee, and H. H. Mantsch.** 1993. Human and rodent Alzheimer beta-amyloid peptides acquire distinct conformations in membrane-mimicking solvents. Eur. J. Biochem. **211:**249–257.
27. **Ozel, M., and H. Diringer.** 1994. Small virus-like structure in fraction from scrapie hamster brain. Lancet **343:**894–895.
28. **Ozel, M., Y.-G. Xi, E. Baldauf, H. Diringer, and M. Pocchiari.** 1994. Small virus-like structure in brains from cases of sporadic and familial Creutzfeldt-Jakob disease. Lancet **344:**923–924.
29. **Pan, K.-M., M. Baldwin, J. Nguyen, M. Gasset, A. Serban, D. Groth, I. Mehlhorn, Z. Huang, R. J. Fletterick, F. E. Cohen, and S. B. Prusiner.** 1993. Conversion of α-helices into β-sheets features in the formation of the scrapie prion proteins. Proc. Natl. Acad. Sci. USA **90:**10962–10966.
30. **Parry, H. B.** 1983. *In* D. R. Oppenheimer (ed.), Scrapie disease in sheep, p. 1–192. Academic Press, New York.
31. **Prusiner, S. B.** 1982. Novel proteinaceous infectious particles cause scrapie. Science **216:**136–144.
32. **Prusiner, S. B.** 1991. Molecular biology of prion diseases. Science **252:**1515–1522.
33. **Prusiner, S. B.** 1994. Inherited prion diseases. Proc. Natl. Acad. Sci. USA **91:**4611–4614.
34. **Prusiner, S. B., D. C. Bolton, D. F. Groth, K. A. Bowman, S. P. Cochran, and M. P. McKinley.** 1982. Further purification and characterization of scrapie prions. Biochemistry **21:**6942–6950.
35. **Prusiner, S. B., S. P. Cochran, D. F. Groth, D. E. Downey, K. A. Bowman, and H. M. Martinez.** 1982. Measurement of the scrapie agent using an incubation time interval assay. Ann. Neurol. **11:**353–358.
36. **Prusiner, S. B., D. Groth, A. Serban, N. Stahl, and R. Gabizon.** 1993. Attempts to restore scrapie prion infectivity after exposure to protein denaturants. Proc. Natl. Acad. Sci. USA **90:**2793–2797.
37. **Prusiner, S. B., D. F. Groth, S. P. Cochran, F. R. Masiarz, M. P. McKinley, and H. M. Martinez.** 1980. Molecular properties, partial purification, and assay by incubation period measurements of the hamster scrapie agent. Biochemistry **19:**4883–4891.
38. **Prusiner, S. B., M. P. McKinley, K. A. Bowman, D. C. Bolton, P. E. Bendheim, D. F. Groth, and G. G. Glenner.** 1983. Scrapie prions aggregate to form amyloid-like birefringent rods. Cell **35:**349–358.
39. **Prusiner, S. B., M. Scott, D. Foster, K.-M. Pan, D. Groth, C. Mirenda, M. Torchia, S.-L. Yang, D. Serban, G. A. Carlson, P. C. Hoppe, D. Westaway, and S. J. DeArmond.** 1990. Transgenetic studies implicate interactions between homologous PrP isoforms in scrapie prion replication. Cell **63:**673–686.
40. **Riesner, D.** 1991. The search for a nucleic acid component to scrapie infectivity. Semin. Virol. **2:**215–226.
41. **Rohwer, R. G., and D. C. Gajdusek.** 1980. Scrapie—virus or viroid: the case for a virus, p. 333–355. *In* A. Boese (ed.), Search for the cause of multiple sclerosis and other chronic diseases of the central nervous system. Verlag Chemie, Weinheim, Germany.
42. **Safar, J., P. P. Roller, D. C. Gajdusek, and C. J. Gibbs, Jr.** 1993. Conformational transitions, dissociation, and unfolding of scrapie amyloid (prion) protein. J. Biol. Chem. **268:**20276–20284.
43. **Safar, J., P. P. Roller, D. C. Gajdusek, and C. J. Gibbs, Jr.** 1994. Scrapie amyloid (prion) protein has the conformational characteristics of an aggregated molten globule folding intermediate. Biochemistry **33:**8375–8383.
44. **Siakotos, A. N., D. C. Gajdusek, C. J. Gibbs, Jr., R. D. Traub, and C. Bucana.** 1976. Partial purification of the scrapie agent from mouse brain by pressure disruption and zonal centrifugation in sucrose-sodium chloride gradients. Virology **70:**230–237.
45. **Sklaviadis, T. K., L. Manuelidis, and E. E. Manuelidis.** 1989. Physical properties of the Creutzfeldt-Jakob disease agent. J. Virol. **63:**1212–1222.
46. **Stahl, N., M. A. Baldwin, D. B. Teplow, L. Hood, B. W. Gibson, A. L. Burlingame, and S. B. Prusiner.** 1993. Structural analysis of the scrapie prion protein using mass spectrometry and amino acid sequencing. Biochemistry **32:**1991–2002.
47. **Tanford, C.** 1980. The hydrophobic effect: formation of micelles and biological membranes. John Wiley & Sons, Inc., New York.
48. **Taylor, J. W., and E. T. Kaiser.** 1987. Structure-function analysis of proteins through the design, synthesis, and study of peptide models. Methods Enzymol. **154:**473–498.
49. **Telling, G. C., M. Scott, J. Mastrianni, R. Gabizon, M. Torchia, F. E. Cohen, S. J. DeArmond, and S. B. Prusiner.** 1995. Prion propagation in mice expressing human and chimeric PrP transgenes implicates the interaction of cellular PrP with another protein. Cell **83:**79–90.
50. **Towbin, H., T. Staehelin, and J. Gordon.** 1979. Electrophoretic transfer of proteins from polyacrylamide gels to nitrocellulose sheets: procedure and some applications. Proc. Natl. Acad. Sci. USA **76:**4350–4354.
51. **Wells, G. A. H., and J. W. Wilesmith.** 1995. The neuropathology and epidemiology of bovine spongiform encephalopathy. Brain Pathol. **5:**91–103.